

## Supporting Information

### **Degradable gelatin-based IPN cryogel hemostat for rapidly stopping deep non-compressible hemorrhage and simultaneously improving wound healing**

Ying Huang <sup>a†</sup>, Xin Zhao <sup>a†</sup>, Zhiyi Zhang <sup>a</sup>, Yongping Liang <sup>a</sup>, Zhanhai Yin <sup>c</sup>,

Baojun Chen <sup>c</sup>, Lang Bai <sup>c</sup>, Yong Han <sup>a</sup>, Baolin Guo <sup>a, b, \*</sup>

<sup>a</sup> *Frontier Institute of Science and Technology, and State Key Laboratory for Mechanical Behavior of Materials, Xi'an Jiaotong University, Xi'an, 710049, China*

<sup>b</sup> *Key Laboratory of Shaanxi Province for Craniofacial Precision Medicine Research, College of Stomatology, Xi'an Jiaotong University, Xi'an 710049, China*

<sup>c</sup> *Department of Orthopaedics, The First Affiliated Hospital of Xi'an Jiaotong University, Xi'an, 710061 China*

\* To whom correspondence should be addressed. Tel.: +86-29-83395340. Fax: +86-29-83395131. E-mail: baoling@mail.xjtu.edu.cn

† These authors contributed equally to this work.

## **Materials and methods**

### **Preparation of gelatin/dopamine cryogels (GT/DA)**

The cryogels were prepared by copolymerization of GT aqueous solution and DA aqueous solution at  $-12\text{ }^{\circ}\text{C}$  using  $\text{NaIO}_4$  as oxidant and EDC/NHS as catalyst system. Firstly, GT was dissolved in deionized (DI) water to form a 5 wt% of GT solution. After the pre-cooled in ice bath, add 0, 0.2, 0.4, 0.6, 0.8 and 1 mL of DA solution (100 mg/mL) into 5 mL of GT solution, respectively. Then 0.5 mL of EDC solution (75 mg/mL) and 0.5 mL of NHS solution (45 mg/mL) were added successively, and the molar ratio of amino group on GT backbone to EDC/NHS was 1: 0.5. Finally, a  $\text{NaIO}_4$  solution (37.6 mg/mL) of triple volume for the DA solution was added to the mixed solution, and the molar ratio of DA to  $\text{NaIO}_4$  was 1: 1, and deionized water was added to supplement the system to 10 mL. The above processes were mixed in an ice bath. After that, the cryogel precursor was transferred into prepared mold (the shape of cryogels depends on the shape of the molds) and placed in a freezer at  $-12\text{ }^{\circ}\text{C}$ . The polymerization was allowed to proceed for 36 h, and the resulting cryogels were thawed. The obtained GT/DA cryogels were purified by immersing in DI water for seven days to remove the unreacted polymer and free DA, and the purified GT/DA cryogels showed no DA leakage ( $< 0.1\%$  DA) when further immersed in DI water. The cryogels were coded as GT<sub>m</sub>/DA<sub>n</sub>, m and n represents concentration (mg/mL) of gelatin and dopamine in cryogel precursor, respectively. For example, GT<sub>25</sub>/DA<sub>8</sub> means that 25 mg of gelatin and 8 mg of dopamine are contained per mL of gelatin precursor. Six cryogels with a constant 2.5 wt% GT concentration and the DA

concentrations varying from 0 to 2, 4, 6, 8, and 10 mg/mL were prepared in this study as shown in Table S5.

### **Characterizations**

X-ray photoelectron spectra (XPS) of gelatin sponge, GT25/DA0 and GT25/DA8 were recorded by VG ESCALAB MK II X-ray photoelectron spectrometer.

The morphologies of the freeze-dried cryogels (including shape-free state, shape-fixed state, and recovered shape from shape-fixed state) were observed using a field emission scanning electron microscope (FEI Quanta FEG 250). Before observation, the surface of the cryogels was sprayed with a gold layer.

The cryogels lyophilized were firstly weighed ( $W_O$ ). Then, they were equilibrated in DI water at room temperature and weighted again ( $W_E$ ). The swelling ratio (SR) was calculated as  $SR = (W_E - W_O)/W_O \times 100\%$ .

### **Mechanical performance**

The mechanical performance of the cryogels was tested by compression test and cyclic compression test using TA rheometer (DHR-2) at room temperature. The cryogels were fabricated as cylindrical shapes with a diameter of 10 mm and height of 10 mm. The freeze-dried cryogels were firstly swollen in DI water, and then the compression test of the wet cryogels was conducted with the maximal compression strain up to 80% at a strain speed was 100  $\mu\text{m/s}$ . For the cyclic compression test, a drop of water was added around the wet cryogels sample on the platform before the test, and then an 80% compression strain was employed to conduct the cyclic compression test. The compression strain was firstly performed up to 80% strain and

then released to 0% strain by using constant compression and release strain rate, which was repeated for 10 times or 50 times.

### **Shape recovery performance**

The shape recovery behavior of the cryogels were measured by previously reported methods with some modifications.<sup>1</sup> In brief, the freeze-dried cryogels (8 mm diameter, with initial length of 10mm ( $L_1$ )) was compressed at a strain rate of 100  $\mu\text{m/s}$  and then hold at this strain for 1 min. The compressed gauge length was set as  $L_2$ . After that, the sample was free of any load for 5 min, a fixed gauge length was measured as  $L_3$ . Then the sample was soaked in water for rehydration for 1 min, and the recovery gauge length was measured as  $L_4$ . The test was performed employing a TA rheometer. The  $L_1$ ,  $L_2$ ,  $L_3$ , and  $L_4$  were measured manually by using rheometer's software to adjust gap distance. The test was cycled for three times. The shape recovery fixity ratio and recovery ratio were calculated according to following equations:

$$\text{Maximum compressive strain: } \varepsilon_m = (L_1 - L_2)/L_1 \times 100\%$$

$$\text{Fixed strain: } \varepsilon_u = (L_1 - L_3)/L_1 \times 100\%$$

$$\text{Recovery strain: } \varepsilon_p = (L_4 - L_3)/L_1 \times 100\%$$

$$\text{Strain fixity ratio: } R_f = \varepsilon_u / \varepsilon_m \times 100\%$$

$$\text{Strain recovery ratio} = \varepsilon_p / \varepsilon_u \times 100\% = (L_4 - L_3) / (L_1 - L_3) \times 100\%$$

### **Volumetric expansion ratio**

The test was measured referring to the reported methods.<sup>1</sup> The lyophilized cryogel's shape was fixed by a compression process as described in the shape recovery behavior test part. The diameter ( $D_1$ ) and length ( $L_1$ ) of the shape-fixed cryogels were

determined. After that, the shape fixed cryogels were as added into water to recover its shape. The diameter ( $D_2$ ) and length ( $L_2$ ) of the shape recovered cryogels were further determined. The volumetric expansion ratio was calculated using the following equation:

$$\text{Volumetric expansion ratio} = ((D_2/2)^2 \times L_2) / ((D_1/2)^2 \times L_1)$$

### **Cytocompatibility**

The cytotoxicity of the cryogels was evaluated by a contacting test method and a leaching pattern assay as we previously reported.<sup>2</sup> In brief, for the contacting test method, the swollen cryogels were firstly cut into disks with diameter of 8 mm and height of 1 mm, and then sterilized by immersing them into 75% alcohol. The complete growth medium was Dulbecco's modified eagle medium (DMEM) (Gibco) supplemented with 10% fetal bovine serum (Gibco),  $1.0 \times 10^5$  U/L penicillin (Hyclone) and 100 mg/L streptomycin (Hyclone). L929 cells were seeded into 48-well plate with cell density of 7500 cells/well. After cultivated for one day, the cryogels disks equilibrated in the culture medium were added into each well and kept the culture medium level slightly lower than the cryogels upper surface to ensure the fine contact between cell and cryogels. After cultured for 24 h, the cell viability under the cryogels was tested by LIVE/DEAD<sup>®</sup> Viability/Cytotoxicity Kit assay. After cultured for 1 day, 3 days and 5 days, respectively, the cell viability under the cryogels were tested by alamarBlue<sup>®</sup> assay. 20  $\mu$ L of alamarBlue<sup>®</sup> reagent in 200  $\mu$ L culture medium was added into each well after removing the cryogels disks and medium. After incubated at 37 °C for 4 h, 100  $\mu$ L of the medium in each well was transferred

to a 96-well black plate (Costar). Fluorescence was read using 560 nm as the excitation wavelength and 600 nm as the emission wavelength by using a microplate reader (Molecular Devices). Cells seeded on TCP without cryogels disc was used as positive control. Tests were repeated four times for each group. Cell adhesion and viability were observed under an inverted fluorescence microscope (IX53, Olympus). For the leaching pattern assay, the sterilized dried cryogels were immersed in the medium for 24 hours at 37 °C with a shaking speed of 100 rpm to obtain the extract solutions, which varied the cryogels concentrations from 20 to 15, 10 and 5 mg/mL in the culture medium. L929 cells were seeded into 96-well plate with cell density of 10000 cells per well, and then replaced the culture medium with cryogels extract solutions after pre-cultured for 24 h. After cultivated for 24 h, the cell viability was tested by alamarBlue<sup>®</sup> assay. The medium was replaced with 10  $\mu$ L of alamarBlue<sup>®</sup> reagent in 100  $\mu$ L complete growth medium. After cultured for 4 h, 100  $\mu$ L of the medium in each well was transferred into a 96-well black plate (Costar). Fluorescence was read using 560 nm as the excitation wavelength and 600 nm as the emission wavelength using a microplate reader (Molecular Devices). Cells seeded on TCP without extract solution were used as positive control group. Tests were repeated eight times for each group.

### **Hemocompatibility**

For hemolytic activity test, erythrocytes were separated from the mouse blood by centrifugation (at 116 $\times$ g) for 10 minutes. The obtained erythrocytes were washed three times with DPBS and then diluted to a concentration of 5% (v/v). Then, the

lyophilized cryogels were dispersed into homogenate by using tissue grinder to form cryogels dispersion liquids with the concentrations varying was 7500, 5000, 2500, 1250 to 625  $\mu\text{g/mL}$ , respectively. 0.5 mL of the dispersion liquid was added into 2 mL tube, and then gently mixed with 500  $\mu\text{L}$  of erythrocyte suspension (5% (v/v)). After incubated at 37 °C for 1 h, the tubes were centrifuged at 116 $\times$ g for 10 minutes, and the supernatants were transferred into new tubes and further centrifuged at 11617 $\times$ g for 10 minutes to exhaustively remove the cryogels particles. The obtained supernatants were introduced into 96-well microplate. The absorbance of the solution was read at 540 nm by a microplate reader (Molecular Devices). 0.1% Triton X-100 was used as the positive control while DPBS was used as the negative control. The hemolysis percentage was calculated as follow: Hemolysis (%) =  $[(A_p - A_b)/(A_t - A_b)] \times 100\%$  where  $A_p$  represented the absorbance value of cryogels supernatant,  $A_t$  represented the absorbance value of Triton X-100 positive control and  $A_b$  was the absorbance value for DPBS. Each group was repeated for three times.

### **Whole blood clotting**

The whole blood clotting test was performed referring to previous report.<sup>3</sup> The cryogels were cut into cylindrical cryogel with a height of 5 mm and a diameter of 10 mm, and then the cylindrical cryogels were formed into shape-fixed situation. A volume of 50  $\mu\text{L}$  of recalcified whole-blood solution (0.2 M  $\text{CaCl}_2$ , 10 mM in the blood) was added onto the pre-warmed cryogels (37 °C) in polypropylene tubes, respectively. Then, the tube was incubated at 37 °C for 30 s, 60 s, 90 s, 120 s, and 150 s, respectively. The gauze and gelatin hemostatic sponge were used as control groups.

After the pre-set period, 10 mL of DI water was gently added to release unbound blood without disturbing the clot. The absorbance of the supernatant was recorded at 540 nm by using a microplate reader (Molecular Devices). Three replicates were performed. The absorbance of 50  $\mu$ L of recalcified whole-blood in 10 mL DI water was used as the reference value (negative control). The blood-clotting index (BCI) was calculated using equation:  $BCI (\%) = (I_s - I_o)/(I_r - I_o) \times 100\%$ . where  $I_s$  represented the absorbance of sample,  $I_r$  represented the absorbance of the reference value and  $I_o$  represented the absorbance of DI water.

### **Blood cell and platelet adhesion**

The blood cell and platelet adhesion tests were conducted referring to references.<sup>3,4</sup> The cryogels were cut into disks with a height of 5 mm and a diameter of 10 mm, and then immersed into DPBS for 1 h at 37 °C. Following that, the ACD-whole blood was added dropwise onto the sample and then incubated for 5 min at 37 °C. Platelet-rich plasma (PRP) was separated from the ACD-whole blood by centrifugation of blood at 116 $\times$ g for 10 min. The PRP was then added dropwise onto the sample and incubated for 1 h at 37 °C. All samples were then washed with DPBS solution three times to remove the physical adhered blood cell and platelet and then fixed by 2.5% glutaraldehyde for another 2 h. After that, blood cells and platelets were dehydrated using 50%, 60%, 70%, 80%, 90%, and 100% ethanol solutions with time interval of 10 min. Finally, the samples were dried and observed using SEM.

### **In vivo hemostatic capacity**

The in vivo hemostatic capacity of the dried cryogels was tested by mouse-tail



amputation model<sup>1, 5</sup>, mouse liver trauma model<sup>1, 6</sup>, rat liver incision model<sup>7</sup> and rabbit liver cross incision model<sup>6, 8</sup> as previously reported methods with some modifications. All animal studies were approved by the animal research committee of Xi'an Jiaotong University.

For the mouse-tail amputation model, the mice (Kunming mice, 5-6-week-old, weighing 32-38 g, female) were randomly and equally divided into nine groups. The animals were anesthetized by injecting 10 wt % chloral hydrate (0.3 mL per 100 g weight of animal) and fixed on a surgical corkboard. Fifty percent length of the tail was cut by surgical scissors. After cutting, the tail of the mouse was placed in air for 15 s to ensure normal blood loss. Then the wound was covered with the preweighted gauze, hemostatic sponge, and shape-fixed cryogels under slight pressure. The data of bleeding time and blood loss were recorded during the hemostatic process. The wound without treatment was used as control group. Each group contains six mice.

For mouse liver trauma model, the mice (Kunming mice, 5-6-week-old, weight 32-38 g, female) were randomly and equally divided into nine groups. The animals were anesthetized by injecting 10 wt% chloral hydrate and fixed on a surgical corkboard. The liver of the mouse was exposed by abdominal incision, and serous fluid around the liver was carefully removed to prevent inaccuracies in the estimation of the blood weight obtained by the hemostatic samples. A pre-weighted filter paper on a paraffin film was placed beneath the liver. Bleeding from the liver was induced using a 16 G needle with the corkboard tilted at about 30°. The preweighted gauze, gelatin hemostatic sponge, and shape-fixed cryogels were immediately applied onto the

bleeding site, respectively. No treatment after pricking the liver was used as control group. The data of bleeding time and blood loss were recorded during the hemostatic process. Each group contains eight mice.

For rat liver incision model, the lyophilized cryogels were compressed as the shape-fixed state for the test. Prewighted gauze and hemostatic sponge, as two commercial hemostatic agents, were used as controls. The SD rats (weight of 180–200 g, female) were randomly and equally divided into nine groups. The animals were anesthetized by injecting 10 wt% chloral hydrate and fixed on a surgical corkboard. The liver of the rat was exposed by abdominal incision, and serous fluid around the liver was carefully removed. Then, a scalpel was used to create a wound that is 8 mm long and 3 mm deep. Immediately after wiping off the blood using gauze, the shape-fixed dried cryogels or commercial hemostatic agent was applied onto the site of lesion. After the performance, the bleeding time and blood loss were recorded accordingly. No treatment after cut the liver was used as control group. Each group contains eight rats.

For rabbit liver cross incision model, the lyophilized GT25/DA0 and GT25/DA8 were compressed as the shape-fixed state for the test. Prewighted gauze and hemostatic sponge, as two commercial hemostatic agents, were used as controls. The New Zealand white rabbit (weight of 1.8–2 kg, male) were randomly and equally divided into five groups. The animals were anesthetized by injecting 10 wt% chloral hydrate and fixed on a surgical corkboard. The liver of the rabbit was exposed by abdominal incision, and serous fluid around the liver was carefully removed. Then, cut by a

scalpel to create a cross-wound that is 10 mm long and 5 mm deep. Immediately after wiping off the blood using gauze, the shape-fixed dried cryogels or commercial hemostatic agent was applied onto the site of lesion. After the performance, the bleeding time and blood loss were recorded accordingly. No treatment after cut the liver was used as control group. Each group contains seven rabbits.

### **Tissue adhesion performance**

The tissue adhesive ability of GT25/DA8 was assessed by liver adhesive stretching test.<sup>9</sup> Briefly, the cylindrical cryogels with the 10 mm diameter and 4 cm length and fixed along the length by compression, then two cryogels were covered in the surface of liver's both ends with no pressure. Finally, the adhesive strength between cryogel and liver was measured by Electro-Mechanical Universal Testing Machines (MTS).

### **In vivo deep narrow non-compressible hemorrhage hemostasis capacity**

The in vivo deep narrow non-compressible hemorrhage hemostasis of the dried cryogels was evaluated by a rabbit liver defect hemorrhage model<sup>1</sup> as we previously reported. The animal experiments were approved by the institutional review board of Xi'an Jiaotong University. The cylindrical lyophilized cryogels (with diameter of 16 mm and height of 8 mm) were compressed as shape-fixed cylindrical cryogels with the diameter of about 9 mm. Then the shape-fixed cryogels were loaded into syringe (with inner diameter of 9 mm and external diameter of 10 mm) for further in vivo injection. Two types of gelatin hemostatic sponges (with a height of 8 mm and diameters of 9 mm and 12 mm, respectively) were used as control groups. New Zealand White rabbits (weight of 1.8–2 kg, male) were fixed on the surgical

cork-board and then 10% chloral hydrate was injected into rabbits enterocoelia to anesthetize them (0.3 mL per 100 g weight of animal). Following that, the rabbit experienced an abdominal incision to expose its liver, the serous fluid around the liver was carefully removed, and then a columniform liver volume defect (with a diameter of 10 mm and height of 5 mm) was made in liver using biopsy needle (inner diameter of 10 mm) and surgical scissors. Immediately after wiping off the blood by using gauze, the cryogels were injected into the defect hole or gelatin hemostatic sponge was inserted into the defect hole. During the hemostatic process, the weighed gauze was used to absorb the flowing blood. The hemostatic time and blood loss were recorded accordingly. Each group contains eight rabbits.

#### **In vivo deep lethal massive non-compressible hemorrhage hemostasis capacity**

The in vivo deep lethal massive non-compressible hemorrhage hemostasis of the dried cryogels was further tested by swine subclavian artery and vein complete transection model<sup>10-12</sup> according to the references. 200 pieces of shape-fixed GT25/DA8 (volume after compression is 0.45 mL; volume expansion ratio is 6.9 (Figure 2k)) were loaded into injector as the injectable hemostatic device while 120 pieces of PVA hemostatic sponge (compressed specification is 2 cm × 1.2 cm × 0.3 cm; after expansion, the specification is 2 cm × 1.3 cm × 2 cm; volume expansion ratio is 7.2) were loaded into injector as the injectable hemostatic device and 20 pieces of gauzes (7.5 cm×5 cm, eight layers) were used as control group to ensure to fill the entire cavity. Control the almost the same compression volume and expansion volume of the cryogels as the PVA sponge. Cross-bred Yorkshire swine (weight about 45 kg, male) were used in this

study, and each group had 3 swine. The swine were fasted for at least 12 h before surgery except for water access. The swine were anesthetized by a combination of xylazine hydrochloride and isoflurane, and the anesthetized swine was first induced by injecting xylazine (1.1 mg/kg) via ear vein, and then 5% isoflurane was inhaled to maintain anesthesia. After anesthesia, a cut-down was performed to expose the right femoral artery and femoral vein. A 6F bore tip catheter was placed in the femoral artery to monitor mean arterial pressure (MAP) and in the femoral vein for fluid replacement/resuscitation. The temperature of the swine was monitored by a rectal thermal probe, and core temperature was maintained at 37 °C to 39 °C with a heating pad. The swine were secured in a dorsal recumbent position with abducted left front leg to allow surgical access to the subclavian vessels. A 4.5 cm skin incision was made above the cranial aspect of the left superficial pectoralis muscle, approximately 5 cm parallel to the sternum. The pectoral muscles were divided to expose the subclavian artery, vein, and brachial nerve plexuses. A 5 cm section of subclavian artery and vein was then dissected free from surrounding tissues. The preinjury wound cavity volume was measured by filling the cavity with a measured volume of warm saline. The vessels were bathed in a 2% lidocaine solution to promote vessel dilation. A 10 minute stabilization period was initiated, which was defined by a stable MAP of more than 65 mm Hg, body temperature at 37 °C to 39 °C, and artery diameter larger than 6 mm. Full transection of the subclavian artery, vein and nerve plexus was then created using surgical scissors at the midaxillary line. The wound was allowed to bleed freely for 30 s. The pretreatment blood loss was defined as the sum

of the following two measurements: (1) amount of blood exiting the cavity during the free bleed and (2) the initial cavity volume. Initial cavity volume was included in pretreatment blood loss to account for the blood that was pooled in the cavity during the free bleed. Both the injectable hemostatic device and gauze were applied to the wound immediately after the free bleeding. Swine were randomized to receive either injectable hemostatic device or gauze treatment. The MAP was monitored during application and at 15 min intervals after the application. Prewarmed Lactated Ringer's solution (LR) (37 °C) was administered for resuscitation to raise the MAP to 65 mm Hg if the MAP was less than 60 mm Hg. When the MAP reached 65 mm Hg or higher, infusion of resuscitation LR was discontinued unless pressure dropped to 60 mm Hg. The time required to fill the wound cavity with hemostatic cryogels, PVA hemostatic sponge or gauze was recorded as the application time. No external pressure was applied to wound after the application of hemostatic device. Press for 3 min to wound after the application of gauze. The 1 h posttreatment observation period began once the manual compression was completed or the cryogels were injected into the wound cavity. After the observation period begins, the wound site was inspected for signs of bleeding. Prospectively identified primary endpoints include posttreatment blood loss and hemostasis time. Any additional blood shed from the wound site was recorded as posttreatment blood loss. For categorical variables, group differences in frequency of response were tested using chi-square test. A significance level of 0.05 was used for all comparisons. As Table S6 showed there was no significant difference between cryogels hemostatic device group, PVA hemostatic sponge and gauze control group

for baseline physiologic measurements.

### **Antioxidant activity**

The antioxidant efficiency of the cryogels were evaluated by the method of scavenging the stable 1, 1-diphenyl-2-picrylhydrazyl (DPPH) free radical.<sup>13</sup> 12 mg of lyophilized cryogels in 2.7 mL of ethyl alcohol was dispersed into homogenate by using tissue grinder to form cryogels dispersion liquid. Afterward, 0.3 mL of 1 mM DPPH in ethyl alcohol was added into the above dispersion liquid. The mixture was stirred and incubated in a dark place for 30 min. Then, the wavelength of DPPH was scanned by a UV-vis spectrophotometer. The degradation of DPPH was calculated by the following equation: DPPH scavenging % =  $(A_b - A_h)/A_b \times 100\%$ . where  $A_b$ ,  $A_h$  are the absorption of the blank (DPPH + ethanol) and the absorption of the sample (DPPH + ethanol + sample), respectively.

### **Photo-thermal performance**

To test the cryogels' photo-thermal property, the swollen cryogels were cut into disks (a diameter of 10 mm and a height of 5 mm) and then exposed to a NIR laser (MDL-III-808nm-1000mW, Changchun New Industries Optoelectronics Tech Co., Ltd.) at a power density of 1.4 W/cm<sup>2</sup> for 10 min. The heat maps and temperature profiles of the cryogels were recorded using an infrared (IR) thermal camera. Besides, the heat maps and temperature profiles of the GT25/DA8 were also conducted at power density varying from 1.0 to 1.4 and 1.8 W/cm<sup>2</sup>, respectively.

### **NIR irradiation assisted antibacterial performance**

The GT25/DA0 and GT25/DA8 disks (with a diameter of 10 mm and height of 5 mm)

were sterilized by immersing them in 75% alcohol and then equilibrated using sterilized DPBS. 10  $\mu\text{L}$  of bacterial suspension in sterilized DPBS ( $10^8$  CFU  $\text{mL}^{-1}$ ) was added onto the surface of the swollen GT25/DA0 and GT25/DA8. After that, the samples were exposed to NIR laser light (808 nm,  $1.4 \text{ W/cm}^2$ ) for different time intervals from 0 to 1, 3, 5 and 10 min, respectively. 10  $\mu\text{L}$  of bacterial suspension ( $10^8$  CFU  $\text{mL}^{-1}$ ) suspended in 200  $\mu\text{L}$  of DPBS was used as a negative control, which was also exposed to NIR laser light (808 nm,  $1.4 \text{ W/cm}^2$ ). 1 mL of sterilized DPBS was introduced into each well to re-suspend any bacterial survivor. Then, 10  $\mu\text{L}$  of the above resuspension was added onto agar plate, the colony-forming units on the agar plate were calculated after cultured for 18 to 24 h at  $37^\circ\text{C}$ . The antibacterial efficiency was expressed as antibacterial ratio using the following equation:

$$\text{Antibacterial ratio (\%)} = ((\text{bacterial count of control} - \text{survivor count on cryogel}) / \text{bacterial count of control}) \times 100\%.$$

### **Controlled release of antibiotic**

For antibiotic encapsulation, 800  $\mu\text{L}$  of vancomycin or doxycycline solution (2.5 mg/mL in deionized water) was dropwise added to 1 mL of lyophilized GT25/DA8, respectively. Then, the drug loaded cryogels were further lyophilized after placing at room temperature for 6 hours. For determining the release profiles of drugs from the cryogels, the drug loaded cryogels were added into 10 mL of tubes and then 4 mL of DPBS (pH=7.4, 0.01 M) was further added. The drug free cryogels were used as blank controls. After reaching the pre-set time point, 1 mL of the release buffer was taken out for further analysis. Then, 1 mL of fresh buffer was added to the tubes to



keep the constant volume. The concentrations of the drugs were determined by the UV–vis spectrophotometer (PerkinElmer Lambda 35). The  $\lambda_{\text{max}}$  of vancomycin was 280 nm, while the  $\lambda_{\text{max}}$  of doxycycline was 351 nm.

### **Antibacterial activity of the antibiotic loaded cryogels**

Antibacterial activity of doxycycline and vancomycin loaded GT20/DA8 was evaluated against *E. coli* (gram-negative) and *S. aureus* (gram-positive) according to the agar diffusion test.<sup>14</sup> The agar plates were inoculated with 100  $\mu\text{L}$  of bacterial suspension ( $10^8$  CFU/mL) by spreading. Following that, the drug-loaded cryogels were cut into cylindrical shape with diameter of 10 mm and height of 5 mm, then placed on the inoculated agar plate. The agar plates were incubated at 37 °C for 24 h. The inhibition zone around each sample was measured and recorded as the antibacterial effect of GT25/DA8. Besides, the samples were then transferred to new inoculated agar plates, cultured at 37 °C for another 24, and then the diameter of the inhibition zone was measured again. The above procedures were repeated until no inhibition zone was observed on the new inoculated agar plates. Drug-free GT25/DA8 was used as control to determine the antibacterial activity of the pure GT25/DA8.

### **In vivo wound healing performance**

The wound healing test was performed as we previously reported.<sup>14, 15</sup> All the animal experiments were approved by the institutional review board of Xi'an Jiaotong University. Mice (female, 30-35 g) were used for the test. Before the surgery, the mice were acclimatized for 1 week. The mice were anesthetized by intraperitoneal injection of 10% chloral hydrate (0.3 mg/kg body weight), and then the dorsal region of mouse

above the tail but below the back was shaved for further surgery. Two full thickness wounds with diameter of 7 mm were made on each side of the mouse midline. One group was dressed by Transparent Film Dressing Frame Style (3M Health Care, USA) and GT25/DA0 + Transparent Film Dressing, one group was dressed by GT25/DA8 + Transparent Film Dressing and Transparent Film Dressing, and the third group was dressed by GT25/DA0 + Transparent Film Dressing and GT25/DA8 + Transparent Film Dressing. For wound area monitoring, on the 3rd, 7th, and 15th day, the mice were performed standard anesthesia procedure, and then the wound area was photographed. Collagen amount was evaluated by estimating hydroxyproline content using a commercial kit. The wound closure area was calculated by Image J.

Wound contraction (%) was calculated using the equation:

$$\text{Wound contraction (\%)} = (\text{area (0 day)} - \text{area (n day)}) / (\text{area (0 day)}) \times 100\%$$

### **Histological analysis**

To evaluate the epidermal regeneration and inflammation in wound area, the collected samples on 3rd, 7th, and 14th day were fixed with 4% paraformaldehyde for 1 hour, embedded in paraffin, and then cross-sectioned to 4  $\mu\text{m}$  thickness slices. The obtained slices were then stained by Haematoxylin-Eosin (Beyotime, China). All slices were analyzed and photographed by microscope (IX53, Olympus, Japan).

### **In vitro biodegradation**

The in vitro degradation test was evaluated referring to previous report methods with some modifications.<sup>16-18</sup> In brief, GT25/DA0 and GT25/DA8 were cut into a cylindrical shape (10 mm diameter, 5 mm thick) to keep the similar weight of each

sample. Each cryogel was weighed ( $W_1$ ) and incubated in 5 mL phosphate buffer solution (PBS) (pH 7.4) containing 40 U/mL collagenase type II and 2 mg/mL amoxicillin at 37 °C and shaken at 100 rpm on an orbital shaker (KS4000i, IKA). The phosphate buffer solution was changed every 2 days at pre-determined harvest times, samples were rinsed with deionized water, lyophilized and weighed ( $W_2$ ). Each group was repeated for three times. The degraded ratio was calculated as:

$$\text{Degraded ratio (\%)} = (W_1 - W_2) / W_1 \times 100\%.$$

### **In vivo biodegradation and in vivo host response**

All the animal experiments were performed according to the guidelines established by the committee on animal research at Xi'an Jiaotong University. All the samples were cut into the same shape and size (diameter of 10 mm and height of 5 mm), sterilized with 75% ethanol, and rinsed in phosphate-buffered saline (PBS) overnight. Rats (female, Sprague Dawley, 200–250 g) were anesthetized by injecting 10% chloral hydrate. A small incision was created in the same area on the back of each rat. The prepared samples were placed into the incision, and then the skin was closed. After 7 days and 28 days, the rats were sacrificed and the testing samples were excised with the adjacent tissues. The obtained material-tissue samples were embedded in paraffin, sectioned, and mounted onto slides. The acute inflammatory response and chronic inflammatory response and degraded degree of cryogels were observed and fiber zone was measured by hematoxylin and eosin (H&E) staining. The stained slides were observed and analyzed by microscopy.

## Results

Table S1. The compositions of the cryogels. The number after GT and DA represents weight (mg) of gelatin and dopamine in per mL cryogel precursor. The molar ratio of amino group on gelatin backbone to EDC/NHS were 1: 0.5 in cryogel precursor.

Cryogel	GT (mg)	DA (mg)	EDC (mg)	NHS (mg)	NaIO <sub>4</sub> (mg)
GT15/DA6	15	6	3.75	2.25	6.77
GT20/DA6	20	6	3.75	2.25	6.77
GT25/DA6	25	6	3.75	2.25	6.77
GT30/DA6	30	6	3.75	2.25	6.77
GT40/DA6	40	6	3.75	2.25	6.77

Table S2. Shape recovery performance of the cryogels.  $S_{mc}$ ,  $R_f$ ,  $R_s$ , and  $T_r$  represent maximum compressive strain, fixing ratio, swelling ratio and recovery time, respectively;  $V_r$  and  $V_f$  represent volume in recovery state and volume in fixing state, respectively.

Cryogel	$S_{mc}$ (%)	$R_f$ (%)	$T_r$ in water (s)	$R_s$ (%)	$V_r$ : $V_f$
GT15/DA6	84.2	100	14.8±0.4	38±4.0	7.4±0.3
GT20/DA6	84.6	99	10.7±0.5	35±2.4	7.8±0.6
GT25/DA6	83.8	97	4.4±0.2	36±1.5	7.1±0.5
GT30/DA6	76.4	87	4.8±0.3	32±3.0	4.0±0.2
GT40/DA6	70.1	79	5.2±0.8	32±1.3	3.5±0.2

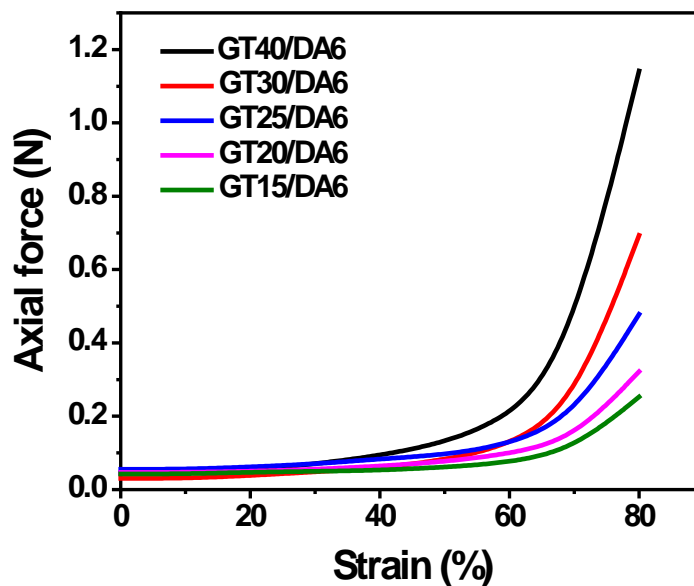


Figure S1. Compression-strain test of the cryogels (8 mm diameter, 10 mm thick) with a 6 mg/mL constant dopamine concentration and varying the gelatin concentration from 15 mg/mL to 20, 25, 30 and 40 mg/mL.

In order to choose a proper gelatin concentration to prepare the GT/DA cryogels, we used a constant dopamine concentration of 6 mg/mL, a constant molar ratio of amino group to EDC/NHS and five different gelatin concentrations varying from 1.5 to 2.0, 2.5, 3.0 and 4.0 wt%, respectively, to prepare five cryogels (Table S2). Then we evaluated the cryogels' compression strength, which gradually increased with the increase of gelatin concentration (Figure S1). Subsequently, we tested the maximum compression ratio, fixing ratio, recovery time, and swelling ratio of the cryogels (Table S3). When the concentration of gelatin was 3 wt% and 4 wt%, the maximum compression ratio was less than 80%, and the fixation ratio was less than 90%, and the shape recovery was not good. When the concentration of gelatin was 1.5 wt% and

2 wt%, the mechanical properties were poor, and the recovery time in the water was greater than 10 s. Therefore, gelatin with a concentration of 2.5 wt% was selected for subsequent test.

Table S3. The compositions of the cryogels. The cryogels are encoded in the form of GT25/DA6-X. The number after GT and DA represents weight (mg) of gelatin and dopamine in per mL cryogel precursor. The X represents molar ratio of EDC/NHS to amino group on gelatin backbone in cryogel precursor.

Cryogel code	GT (mg)	DA (mg)	EDC (mg)	NHS (mg)	NaIO <sub>4</sub> (mg)
GT25/DA6-0.25	25	6	1.875	1.125	6.77
GT25/DA6-0.5	25	6	3.75	2.25	6.77
GT25/DA6-0.75	25	6	5.625	3.375	6.77
GT25/DA6-1	25	6	7.5	4.5	6.77

Table S4. Shape recovery performance of the cryogels.  $S_{mc}$ ,  $R_f$ ,  $R_s$ , and  $T_r$  represent maximum compressive strain, fixing ratio, swelling ratio and recovery time, respectively;  $V_r$  and  $V_f$  represent volume in recovery state and volume in fixing state, respectively.

Cryogel	$S_{mc}$ (%)	$R_f$ (%)	$T_r$ in water (s)	$R_s$ (%)	$V_r:V_f$
GT25/DA6-0.25	83.5	97	13.2±1.0	37±0.8	7.0±0.9
GT25/DA6-0.5	83.8	97	4.4±0.2	36±1.5	7.1±0.5
GT25/DA6-0.75	80.6	93	5.8±1.2	33±2.5	5.6±0.3
GT25/DA6-1	76.3	90	5.1±0.7	34±0.9	3.9±0.6

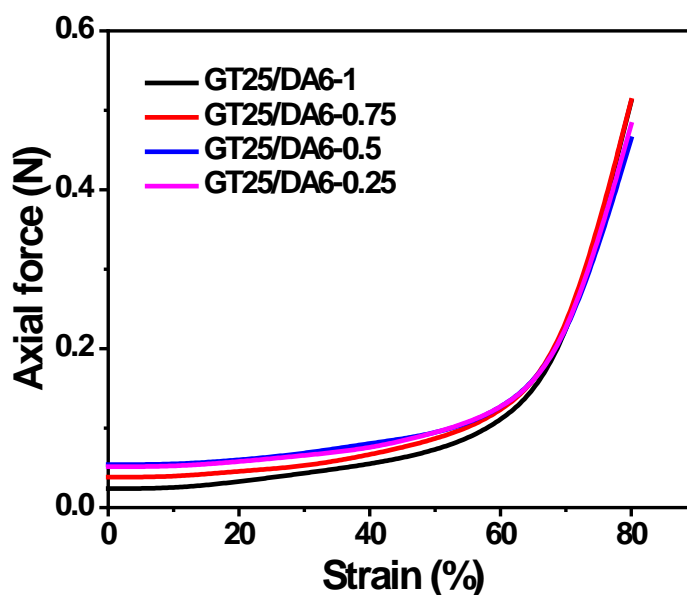


Figure S2. Compression-strain test of the cryogels (8 mm diameter, 10 mm thick) with the GT25/DA6-1, GT25/DA6-0.75, GT25/DA6-0.5 and GT25/DA6-0.25.

In order to choose a proper molar ratio of amino group to EDC/NHS to prepare the GT/DA cryogels, we used a constant dopamine concentration of 6 mg/mL, a constant gelatin concentration of 2.5 wt% and four different molar ratio of amino group to EDC/NHS varying from 1: 0.25, 1: 0.5, 1: 0.75 and 1: 1 respectively, to prepare four cryogels (Table S4). Then we evaluated the cryogels' compression strength, which remained constant with the increase of EDC/NHS concentration (Figure S2). Subsequently, we tested the maximum compression ratio, fixing ratio, recovery time, and swelling ratio of the cryogels (Table S5). It has been found that molar ratio of amino group to EDC/NHS was 1:0.5 that has the best maximum compression ratio and fixed ratio, and can recover the fastest in water. Therefore, the choice of molar ratio of amino group to EDC/NHS was 1:0.5 for subsequent test.

Table S5. The compositions of the cryogels. The number after GT and DA represents weight (mg) of gelatin and dopamine in per mL cryogel precursor, the molar ratio of amino group on gelatin backbone to EDC/NHS were 1: 0.5 in cryogel precursor.  $S_{mc}$  and  $R_f$  represent maximum compressive strain and fixing ratio.

Cryogel	GT (mg)	DA (mg)	EDC (mg)	NHS (mg)	NaIO <sub>4</sub> (mg)	$S_{mc}$ (%)	$R_f$ (%)
GT25/DA0	25	0	3.75	2.25	0	86.6	99
GT25/DA2	25	2	3.75	2.25	2.26	86.2	99
GT25/DA4	25	4	3.75	2.25	4.51	85.6	98
GT25/DA6	25	6	3.75	2.25	6.77	83.8	97
GT25/DA8	25	8	3.75	2.25	9.02	82.3	95
GT25/DA10	25	10	3.75	2.25	11.28	78.9	89

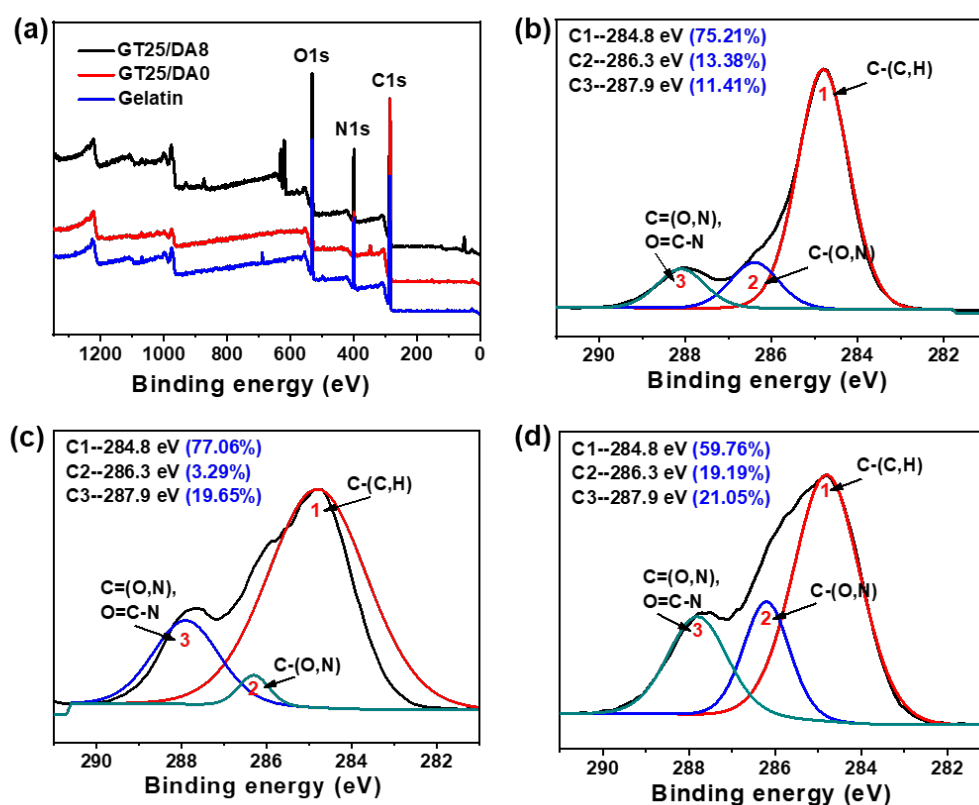


Figure S3. XPS analysis of gelatin, GT25/DA0 and GT25/DA8<sup>19</sup>: (a) XPS survey spectrum; (b) C1s spectrum of gelatin; (c) C1s spectrum of GT25/DA0; (d) C1s spectrum of GT25/DA8.



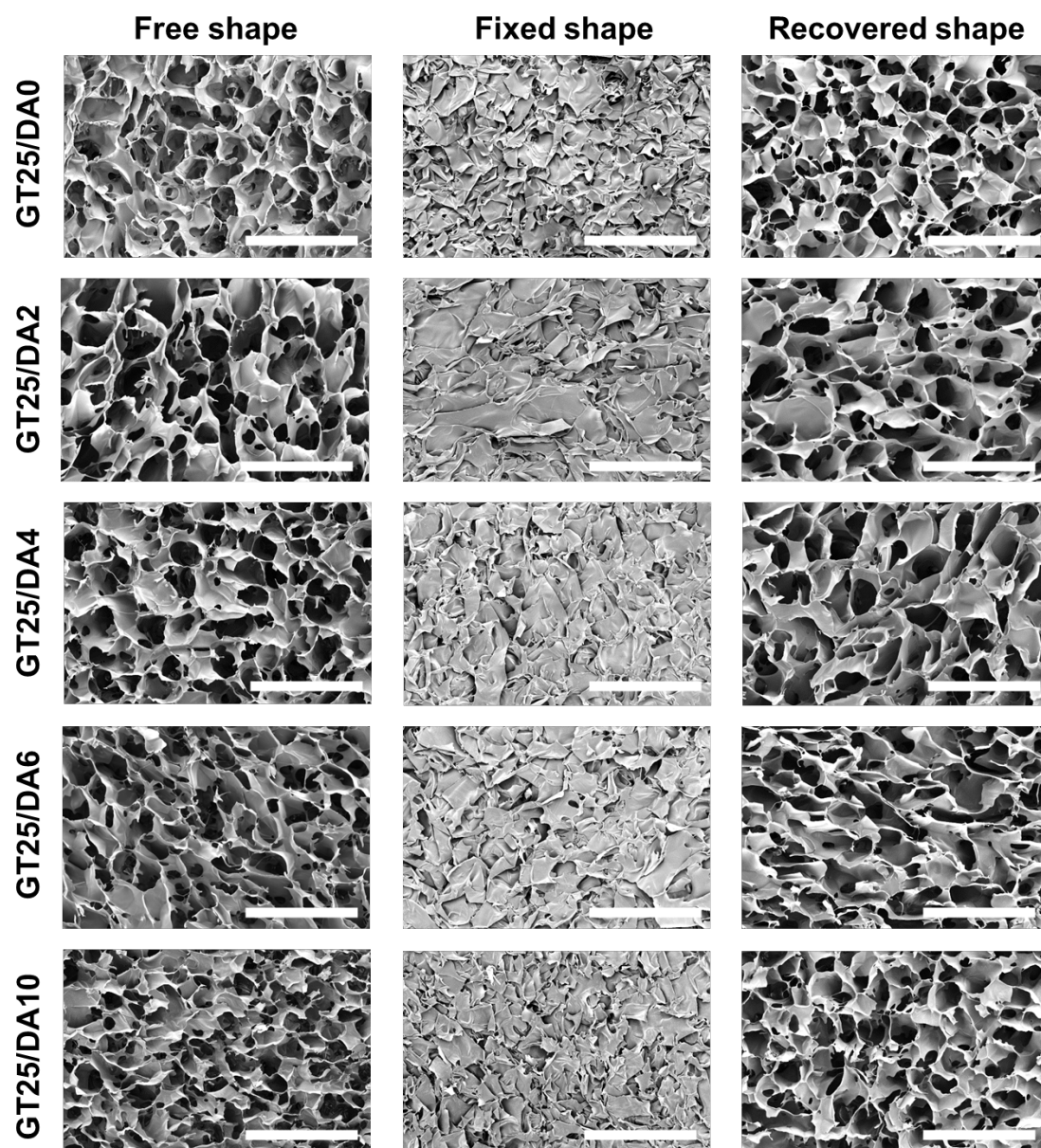


Figure S4. Microtopography of the cryogels in free shape, fixed shape and recovered shape. Scale bar: 300  $\mu\text{m}$ .

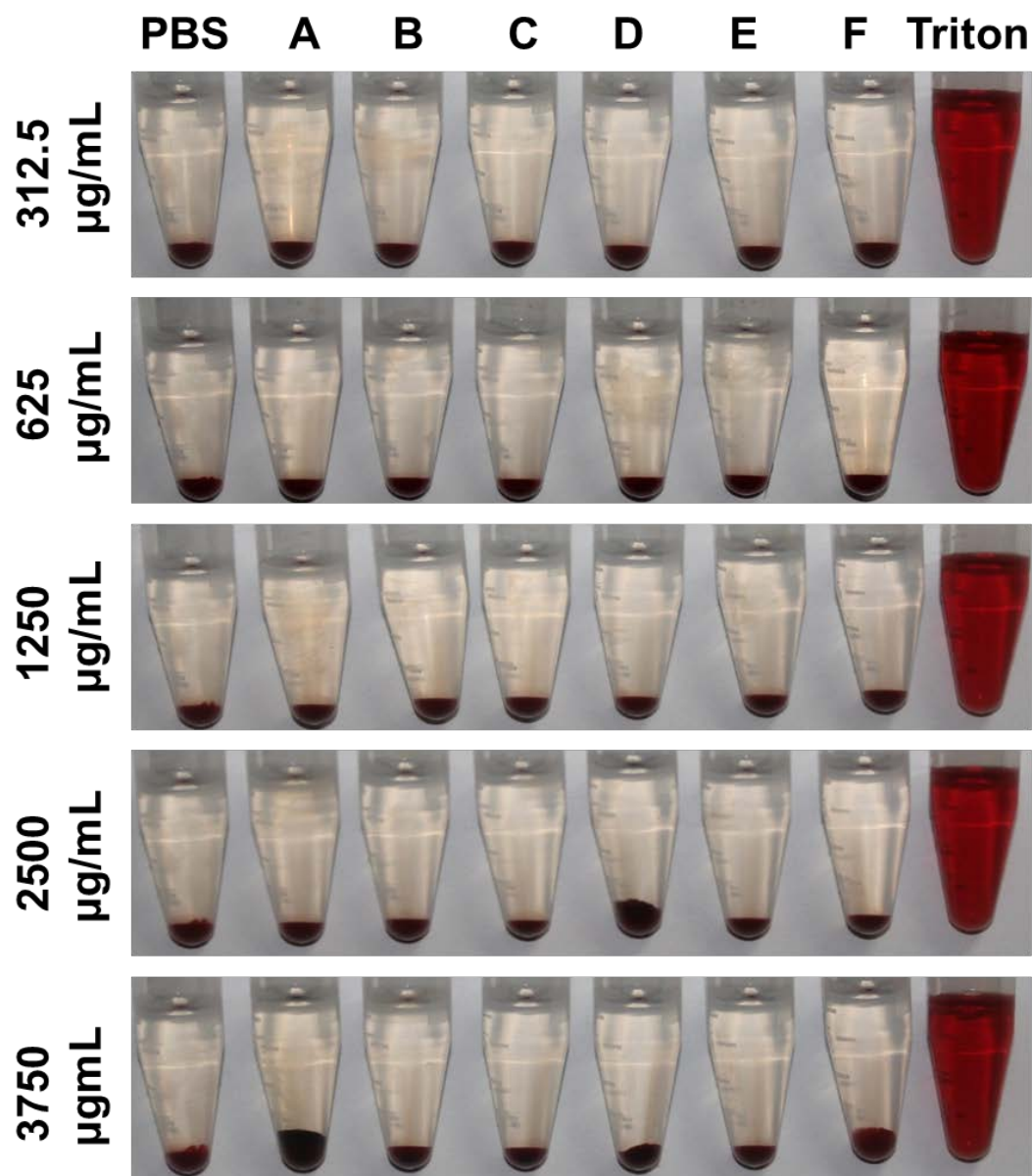


Figure S5. Photographs from hemolytic activity assay of the cryogels using PBS as negative control and Triton X-100 as positive control. A for GT25/DA10, B for GT25/DA8, C for GT25/DA6, D for GT25/DA4, E for GT25/DA2 and F for GT25/DA0.

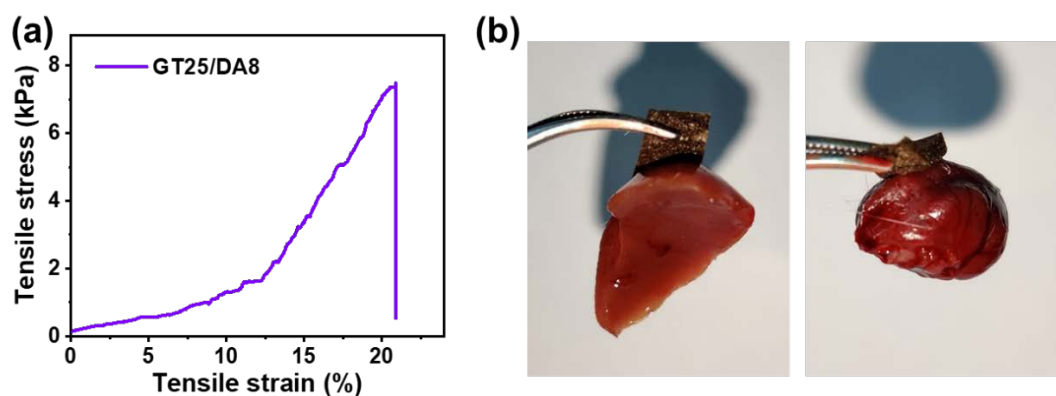


Figure S6. (a) The liver adhesion stretching property of GT25/DA8; (b) The photographs of GT25/DA8 adhered onto biological tissues including liver and heart.

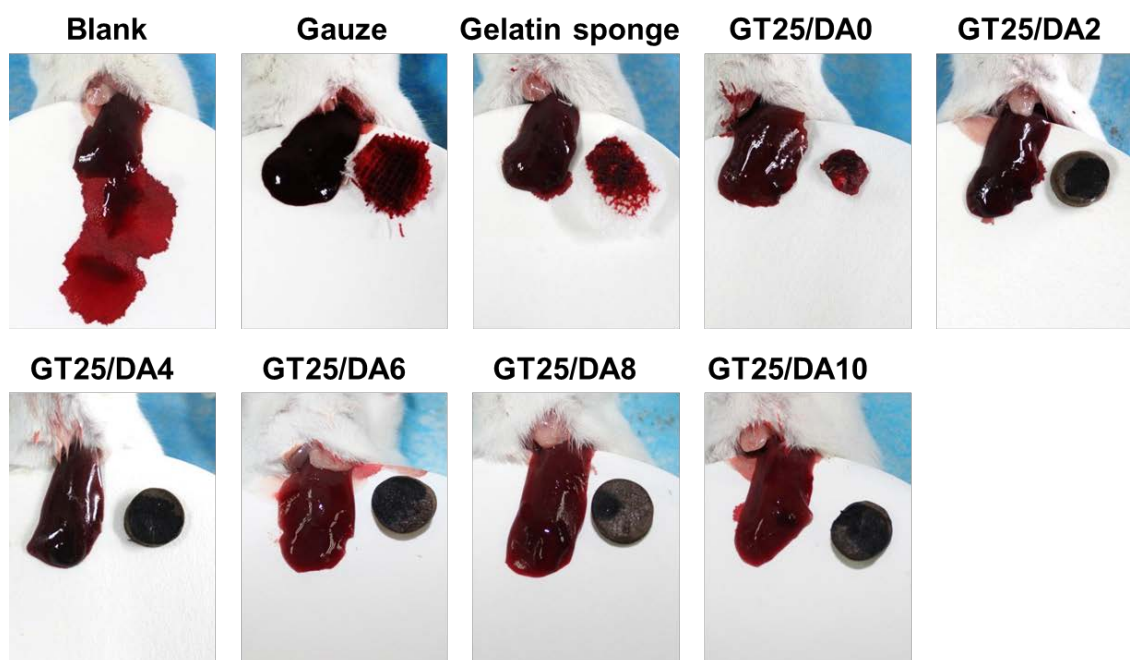


Figure S7. Photographs of the hemostatic agents and blank groups after in vivo hemostasis when using the mouse liver trauma model.

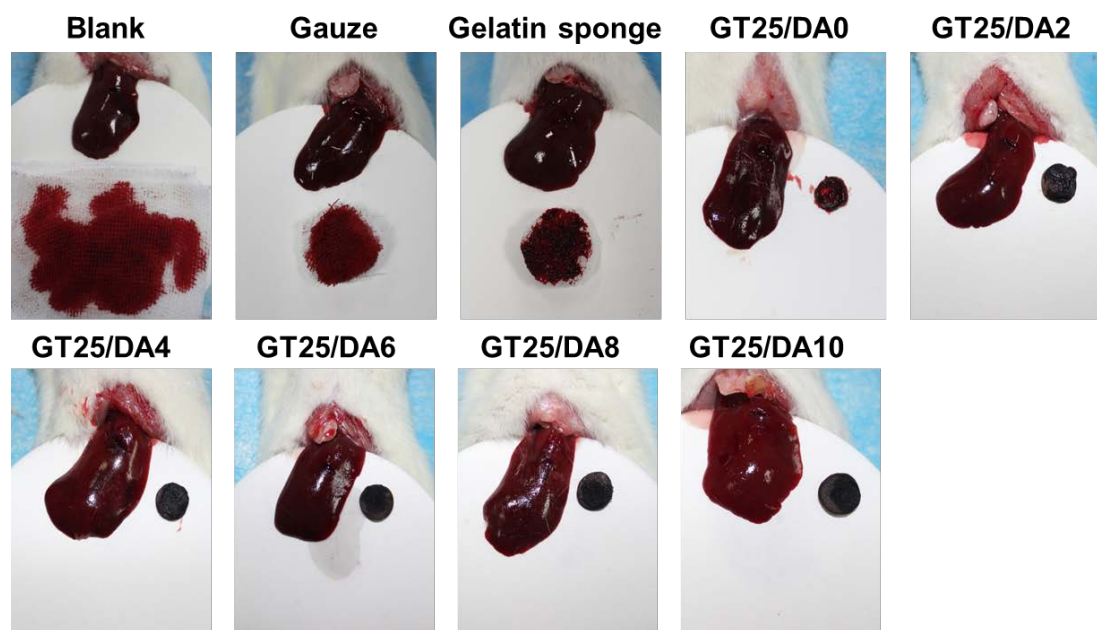


Figure S8. Photographs of the hemostatic agents and blank groups after in vivo hemostasis when using the rat liver incision model.

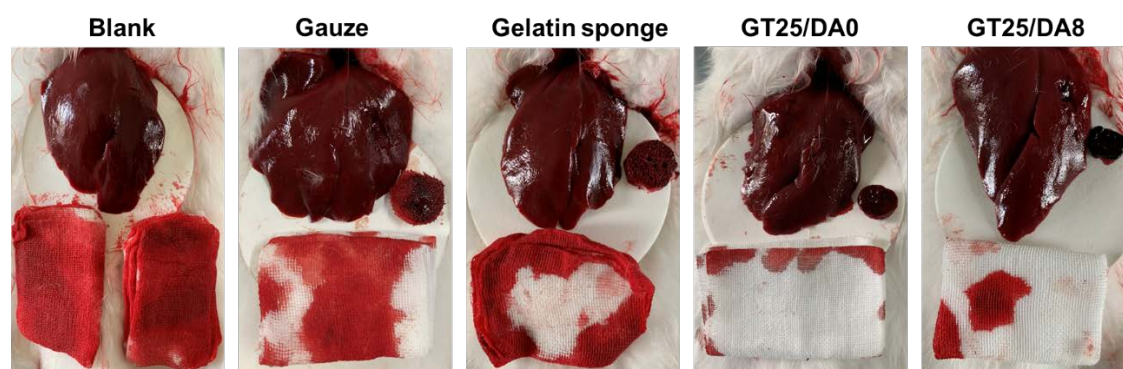


Figure S9. Photographs of the hemostatic agents and blank groups after in vivo hemostasis when using the rabbit liver cross incision model.



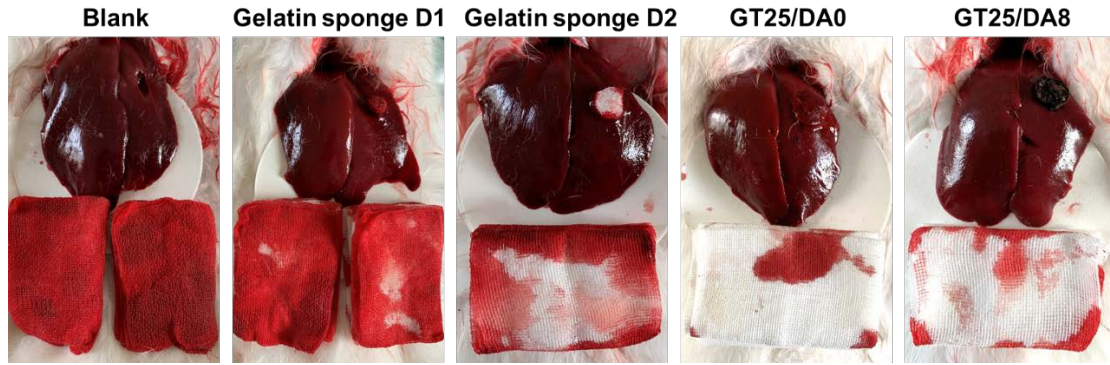


Figure S10. Photographs of the hemostatic agents and blank groups after in vivo hemostasis when using the rabbit liver defect non-compressible hemorrhage model.

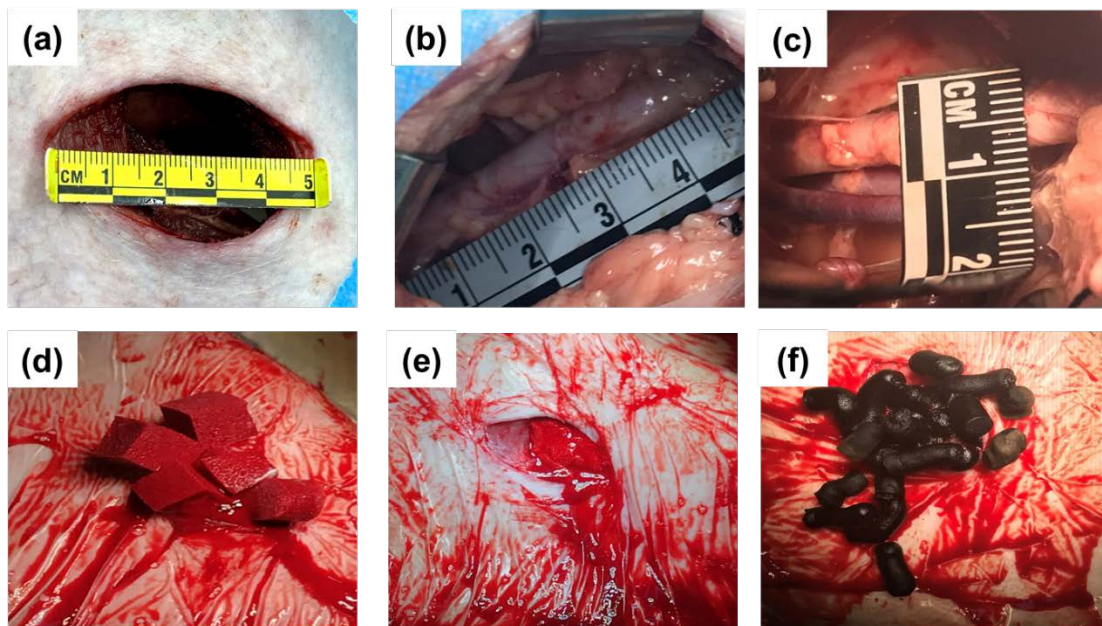


Figure S11. (a) Photograph of the external situation of the wound cavity; (b) Photograph of measuring the length of subclavian artery and vein; (c) Photograph of measuring the diameter of subclavian artery; (d) Photograph of the wound situation after applying the PVA hemostatic sponge for 5 min; (e) Photograph of the wound situation after applying the gauzes for 5 min; (f) Photograph of the wound situation after applying the GT25/DA8 for 5 min.

Table S6. The baseline physiologic measurements, resuscitation fluid volume, oxygen saturation, and MAP at termination of the swine in hemostatic GT25/DA8 group, PVA hemostatic sponge group and gauze group.

Measurement	PVA sponge	Gauze	Cryogel
Swine weight, kg	44.3±3.1	43.7±1.5	44.5±1.3
Oxygen saturation before cutting vessel, %	93.0±3.6	93.0±2.0	92.7±2.3
MAP before cutting vessel, mm Hg	105.3±8.1	104.7±18.4	102.0±13.5
Artery diameter, mm	6.5±0.2	6.4±0.4	6.5±0.4
Preinjury cavity volume, mL	110.0±10.0	105.0±18.0	111.7±20.2
Application time, s	23.7±3.8 <sup>a</sup>	45.3±6.8 <sup>b</sup>	26.3±6.0 <sup>a</sup>
Pretreatment blood loss, mL	531.3±57.2	548.0±102.3	549.7±22.5
Resuscitation fluid volume, mL	1103.3±267.6 <sup>a</sup>	923.3±196.6 <sup>a</sup>	486.7±70.2 <sup>b</sup>
Oxygen saturation at termination, %	94.7±4.5	94.0±5.3	92.7±1.5
MAP at termination, mm Hg	70.7±8.4	68.3±4.7	67.7±5.5

Note: Marked with different lowercase letters indicates significant difference ( $P<0.05$ ); unmarked letters or the same lowercase letters indicate that the difference is not significant ( $P>0.05$ ).

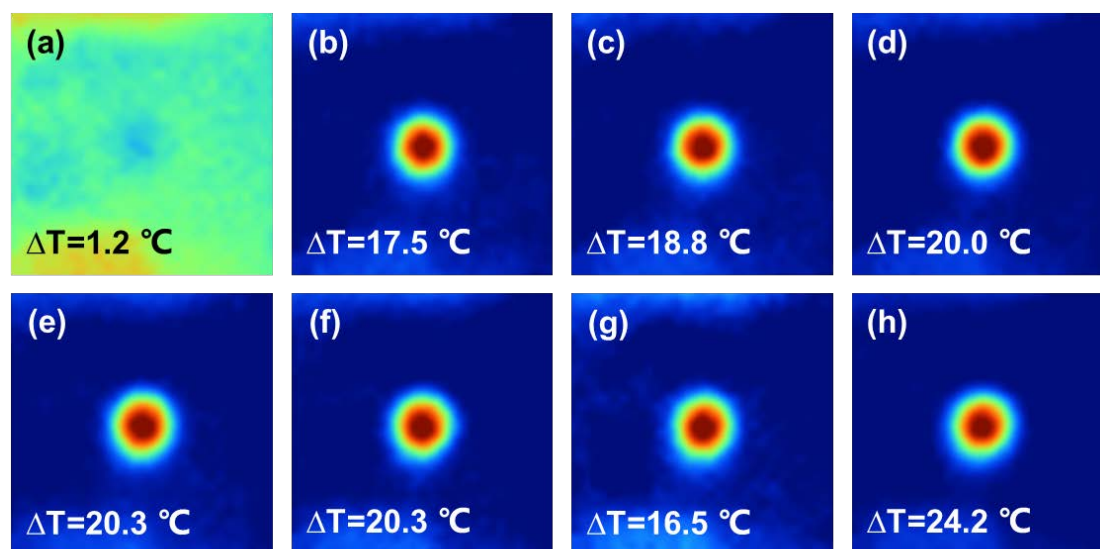


Figure S12. Heat maps of the GT25/DA0 (a), GT25/DA2 (b), GT25/DA4 (c), GT25/DA6 (d), GT25/DA8 (e), and GT25/DA10 (f) after 10 min NIR 808 nm irradiation with a constant light intensity of 1.4 W/cm<sup>2</sup>; Heat maps of GT25/DA8 after 10 min NIR 808 nm irradiation with the light intensity varying from 1.0 (g) to 1.8 (h)

W/cm<sup>2</sup>.

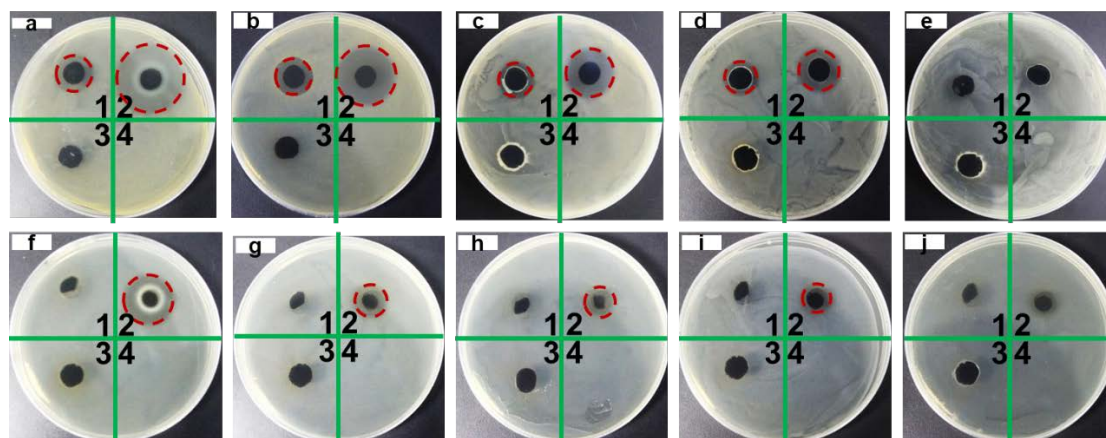


Figure S13. Photographs of survival *S. aureus* (a for 1st day, b for 5th day, c for 9th day, d for 13th day and e for 17th day) and survival *E. coli* (f for 1st day, g for 2nd day, h for 3rd day, i for 4th day and j for 5th day) from agar diffusion test. 1: vancomycin loaded GT25/DA8, 2: doxycycline loaded GT25/DA8, 3: GT25/DA8 and 4: blank.

### Legend for Movie

Movie S1. Process of injecting the shape-fixed GT25/DA8 into the “deep wound” to recover shape and stopping non-compressible hemorrhage.

Movie S2. Shape recovery of the GT25/DA0 and GT25/DA8 after absorbing the water.

### References:

- (1) Zhao, X.; Guo, B. L.; Wu, H.; Liang, Y. P.; Ma, P. X., Injectable antibacterial conductive nanocomposite cryogels with rapid shape recovery for noncompressible hemorrhage and wound healing. *Nat. Commun.* **2018**, 9, 2784.
- (2) Deng, Z. X.; Hu, T. L.; Lei, Q.; He, J. K.; Ma, P. X.; Guo, B. L.,

Stimuli-responsive conductive nanocomposite hydrogels with high stretchability, self-healing, adhesiveness, and 3D printability for human motion sensing. *ACS Appl. Mater. Interfaces* **2019**, 11, (7), 6796-6808.

(3) Quan, K. C.; Li, G. F.; Tao, L.; Xie, Q.; Yuan, Q. P.; Wang, X., Diaminopropionic acid reinforced graphene sponge and its use for hemostasis. *ACS Appl. Mater. Interfaces* **2016**, 8, (12), 7666-7673.

(4) Cheng, F.; Liu, C. Y.; Wei, X. J.; Yan, T. S.; Li, H. B.; He, J. M.; Huang, Y. D., Preparation and characterization of 2,2,6,6-tetramethylpiperidine-1-oxyl (TEMPO)-oxidized cellulose nanocrystal/alginate biodegradable composite dressing for hemostasis applications. *ACS Sustainable Chem. Eng.* **2017**, 5, (5), 3819-3828.

(5) Liu, Y.; Jennings, N. L.; Dart, A. M.; Du, X. J., Standardizing a simpler, more sensitive and accurate tail bleeding assay in mice. *World. J. Exp. Med.* **2012**, 2, (2), 30-6.

(6) Zhao, D. W.; Tian, M.; Yang, J. Z.; Du, P.; Bi, J.; Zhu, X. J.; Li, T., Hemostatic mechanism underlying microbubble-enhanced non-focused ultrasound in the treatment of a rabbit liver trauma model. *Exp. Biol. Med.* **2017**, 242, (2), 231-240.

(7) Wu, J. Q.; Lemarie, C. A.; Barralet, J.; Blostein, M. D., Amphiphilic peptide-loaded nanofibrous calcium phosphate microspheres promote hemostasis in vivo. *Acta Biomater.* **2013**, 9, (11), 9194-9200.

(8) Zhao, X. C.; Li, L.; Zhao, H. Z.; Li, T.; Wu, S. Z.; Zhong, Y.; Zhao, Y.; Liu, Z., Liver haemostasis using microbubble-enhanced ultrasound at a low acoustic intensity. *Eur. Radiol.* **2012**, 22, (2), 379-386.



- (9) Zhao, Y.; Li, Z. H.; Song, S. L.; Yang, K. R.; Liu, H.; Yang, Z.; Wang, J. C.; Yang, B.; Lin, Q., Skin-inspired antibacterial conductive hydrogels for epidermal sensors and diabetic foot wound dressings. *Adv. Funct. Mater.* **2019**, 29, (31), 1901474.
- (10) Arnaud, F.; Parreno-Sadalan, D.; Tomori, T.; Delima, M. G.; Teranishi, K.; Carr, W.; McNamee, G.; McKeague, A.; Govindaraj, K.; Beadling, C.; Lutz, C.; Sharp, T.; Mog, S.; Burris, D.; McCarron, R., Comparison of 10 hemostatic dressings in a groin transection model in swine. *J. Trauma Acute Care Surg.* **2009**, 67, (4), 848-855.
- (11) Devlin, J. J.; Kircher, S.; Kozen, B. G.; Littlejohn, L. F.; Johnson, A. S., Comparison of ChitoFlex®, CELOX™, and QuikClot® in control of hemorrhage. *J. Emerg. Med.* **2011**, 41, (3), 237-245.
- (12) Mueller, G. R.; Pineda, T. J.; Xie, H. X.; Teach, J. S.; Barofsky, A. D.; Schmid, J. R.; Gregory, K. W., A novel sponge-based wound stasis dressing to treat lethal noncompressible hemorrhage. *J. Trauma Acute Care Surg.* **2012**, 73, S134-S139.
- (13) Qu, J.; Zhao, X.; Ma, P. X.; Guo, B. L., Injectable antibacterial conductive hydrogels with dual response to an electric field and pH for localized "smart" drug release. *Acta Biomater.* **2018**, 72, 55-69.
- (14) Liang, Y. P.; Zhao, X.; Hu, T. L.; Chen, B. J.; Yin, Z. H.; Ma, P. X.; Guo, B. L., Adhesive hemostatic conducting injectable composite hydrogels with sustained drug release and photothermal antibacterial activity to promote full-thickness skin regeneration during wound healing. *Small* **2019**, 15, (12), 1900046.
- (15) He, J.; Liang, Y.; Shi, M.; Guo, B., Anti-oxidant electroactive and antibacterial nanofibrous wound dressings based on poly( $\epsilon$ -caprolactone)/quaternized

chitosan-graft-polyaniline for full-thickness skin wound healing. *Chem. Eng. J.* **2020**, 385, 123464.

(16) Koshy, S. T.; Ferrante, T. C.; Lewin, S. A.; Mooney, D. J., Injectable, porous, and cell-responsive gelatin cryogels. *Biomaterials* **2014**, 35, (8), 2477-2487.

(17) Wu, Y.; Wang, L.; Guo, B.; Shao, Y.; Ma, P. X., Electroactive biodegradable polyurethane significantly enhanced Schwann cells myelin gene expression and neurotrophin secretion for peripheral nerve tissue engineering. *Biomaterials* **2016**, 87, 18-31.

(18) Li, M.; Chen, J.; Shi, M.; Zhang, H.; Ma, P. X.; Guo, B., Electroactive anti-oxidant polyurethane elastomers with shape memory property as non-adherent wound dressing to enhance wound healing. *Chem. Eng. J.* **2019**, 375, 121999.

(19) Tayefeh, A.; Poursalehi, R.; Wiesner, M.; Mousavi, S. A., XPS study of size effects of Fe<sub>3</sub>O<sub>4</sub> nanoparticles on crosslinking degree of magnetic TFN membrane. *Polym. Test.* **2019**, 73, 232-241.